Vafeas, A. T., Fafoutis, X., Elsts, A., Craddock, I. J., Biswas, M. I., Piechocki, R. J., & Oikonomou, G. (2020). *Wearable Devices for Digital Health: The SPHERE Wearable 3*. Paper presented at Embedded Wireless Systems and Networks (EWSN), Lyon, France.

Peer reviewed version

Wearable Devices for Digital Health: The SPHERE Wearable 3

Antonis Vafeas, Md Israfil Biswas
Electrical and Electronic Engineering
University of Bristol, UK

Xenofon Fafoutis
DTU Compute
Technical University of Denmark

Atis Elsts
Institute of Electronics and Computer Science (EDI)

Ian Craddock
Electrical and Electronic Engineering
University of Bristol, UK

Robert Piechocki
Electrical and Electronic Engineering
University of Bristol, UK

George Oikonomou
Electrical and Electronic Engineering
University of Bristol, UK

Abstract

This paper presents a novel wearable device: the SPHERE Wearable 3. The Wearable 3 is a wrist-worn sensor node tailored for low maintenance residential health and behaviour monitoring. It features multiple inertial measurement sensors, as well as a heart-rate sensor, capacitive button, and OLED screen. The Wearable 3 builds on our experience with previous generations of wearable sensing nodes while adding novel features, including interactive elements. We present a novel two-way communication based on a customized implementation of the Bluetooth Low Energy (BLE) protocol to connect the Wearable 3 with a gateway device, and describe various optimizations of energy consumption. The Wearable 3 is currently being deployed in residential homes in Bristol, UK, as part of a project aiming to collect diagnostic data from early-stage Alzheimer's patients.

1 Introduction

Internet of Things (IoT) poses to revolutionize the healthcare provision with the advances in sensing technology and microelectronics. This is especially important as our health systems are challenged by increasing chronic illness. The long-term sustainability of health care must be improved by early detection of medical conditions to enable cost-effective and personalized treatment.

With the rapid development of wearable technologies [10], monitoring their own well-being can encourage people to facilitate timely interventions, as well as enable better diagnostics and research through long-term activity monitoring. One example of this is the SPHERE project. SPHERE (a Sensor Platform for Healthcare in a Residential Environment) is an interdisciplinary research collaboration that aims to monitor the everyday behaviour of the users in their home environment [7].

However, such a long-term activity monitoring in a residential environment requires that the wearables have low energy consumption and achieve efficient channel utilization. The devices are also expected to require minimum maintenance (such as recharging or replacement of batteries). In this paper we preset the Wearable 3: the third version of the SPHERE Wearable sensor nodes. The Wearable 3 extends our previous work [7, 8] on SPW-1 (SPHERE Wearable 1) and SPW-2 (SPHERE Wearable 2) and builds up on our experience when applying these nodes for human monitoring in the home environment. Our contributions are:

- We describe the system architecture of the SPHERE Wearable 3;
- We demonstrate better energy consumption per radio utilization;
- We demonstrates better channel utilization with bidirectional information exchange;
- We quantify the performance of the new wearable.

The Wearable 3 is currently used as part of the SPHERE multimodal sensor platform [5] in residential installations in the CUBOiD project. The objective of CUBOiD is to develop novel behavioural analysis algorithms for dementia-related diagnostic signatures, enabling early diagnostics and new therapies of people with early-stage Alzheimer's disease. To this end, it is especially important the the Wearable 3 is easy-to-use as well as aesthetically pleasing.

2 Related Work

The research community has conducted a large number of experiments regarding wearable devices for activity monitoring.

The advancement in microelectronics and the recent developments in commercial wearable devices (e.g., Nike+ Fuelband SE, Jawbone UP etc.) have led to an explosive growth in number of wearables used as fitness trackers and smartwatches. In [11], a literature survey on the legitimacy, suitability and adequacy of wearable technology in the fields

of personal health informatics, behaviour change, and medical support is presented. The wearable devices are equipped with advance sensors (e.g., accelerometers, GPS, heart rate monitors etc.) for personal health monitoring or fitness support.

However, a new framework for these wearable gadgets is required because of the limited access of the raw data. The new framework will overcome the limited use of such devices for research or medical applications. Their lack of interoperability with other healthcare systems and their limited expandability to new sensor technologies will be opened through the new platform. Additionally, research for the new framework will help to manage the need for regular recharging of these devices depending on the target groups that are uncomfortable with or physically unable of managing modern technologies. For example, gadgets with typical battery lifetime of less than a week can hampers their fitness for highly sensitive users.

An Ambient Assisted Living (AAL) platform called Verity is presented in [13] based on psychological signal monitoring that helps to provide original health evidence from the human body using accelerometer and a piezo-resistive sensor. A Mobile healthcare (mHealth) system depending on biomedical signal monitoring was introduced in in [2] for telemedicine using smartphones and wearable devices. The proposed Data Acquisition Module (DAQ) collects and forward biomedical signals over the Internet for monitoring. A real time monitoring system (PsychoFIZZ) to examine psychological behaviours using various on body sensors (e.g., piezo-resistive, epidermal electrocardiogram (ECG) sensors etc.) is presented in [3] and developed a generic filter library for the system. The system communicates with multiple Digital Sample Units (DSUs) by filtering and interpreting the data to enhance the performance of the system.

Another AAL platform based on a wrist-worn accelerometer by applying Relief-F filter-based approach to select accelerometer features for activity recognition is presented in [9]. The wearable accelerometer is able to identify basic activities, such as sitting, walking, running and jumping but did not report how to recognize standing and sleeping.

A combination of accelerometer and electromyography was considered in [4] to perform identification of basic activities of the elderly and patients. The proposed method uses Zigbee wireless protocol to send the information of the force and accelerometer sensors that claimed 98 % recognition accuracy. The force sensor fusion is used to detect, locate, and track elderly people and the accelerometer decision were merged efficiently to detect the basic activity such as standing, sitting, walking, falling, lying down, and the transitions between their activities. The drawback with this method is, it is costly and consumes a large amount of power for the large numbers of accelerometer and force sensors.

3 System Architecture

The Wearable 3 features the following main components:

- Highly energy-efficient MC3635 accelerometer, with 14 Hz, 28 Hz, 54 Hz and 105 Hz sampling rates
- ICM-20948 nine-axial inertial measurement unit with high-speed sampling accelerometer, gyroscope and magnetometer
- OLED screen
- Capacitive touch button
- 8 MB flash memory
- BQ51013B Qi wireless charger
- CC2650 System-on-Chip with BLE and IEEE 802.15.4 radio.

The Wearable 3 runs the Contiki-NG and Texas Instruments RTOS operating systems.

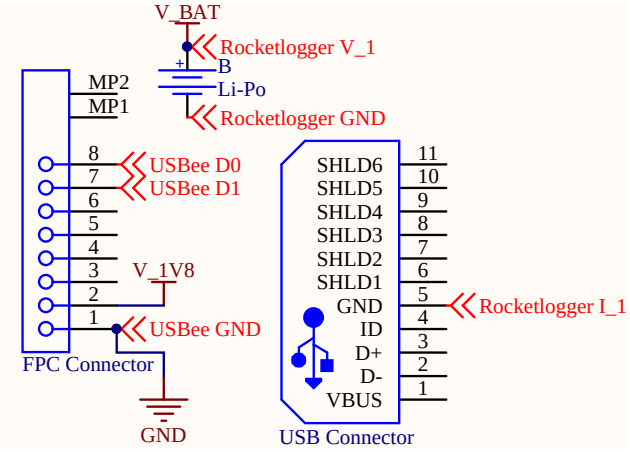

Figure 1. Logic analyzer and Rocketlogger connection schematic.

Fig. 1 shows the setup for experiments. A USBee SX 24Msps logic analyzer was used to measure GPIO pin changes triggered in software. Rocketlogger [12] voltage and current readings together with GPIO changes were recorded. All devices were powered by isolated power supplies and data was collected over isolated Ethernet switches. The logic analyzer provided accurate timings for the different states of the radio at different packet lengths during reception and transmission. The accuracy was verified to 1% error when the byte transmission duration was calculated very close to the theoretical 1Msps or 125 Kbps or 8μs. For the Rocketlogger the voltage channels can provide very accurate readings. However current readings exhibit some variability and inaccuracy during transients. This was accounted for when generating results by oversampling and providing confidence intervals for the results. The on-board FPC connector to provide access to GPIO signals and voltage rails which enabled the data collections and debugging in general. The logic analyzer was connected using extension boards to that connector and set at 24 Msps. Using sigrok and averaging over multiple frames using the timings between GPIO transitions were measured. The analyzing and averaging of the data was undertaken on the exported Value Change Dump (VCD) files. The Rocketlogger data was set to generate in excess of 10 million samples at 64 Ksps having more than 500 thousand traces of transmission or reception. The large quantities of traces were collected to mitigate two limitations. The first one is that Rocketlogger was not synchronized with the debug signals on the GPIOs. The second

one, is that the sampling rate of the Rocketlogger is much lower than the logic analyzer. Those traces will have different time drift with the debug signals. Thus for every trace the samples trail were taken with a different time offset from the debug signals. By averaging out over those complete traces both limitations are accounted for. Our previous work is focused on SPW-1 and SPW-2, the first and second wearable platform of SPHERE, which are presented in Section 3.1. Section 3.2 extends our previous work, introducing the third wearable platform of SPHERE, named Wearable 3.

3.1 SPHERE Previous Generation Wearable Devices

There were two previous generations prior to the device presented in this paper. Generation one, SPW-1 was based on a different microcontroller the nRF51822. The main difference of that particular IC to the current one is the presence of a single ARM Cortex M0 processor compared to a combination of a Cortex M0 and M3 in both the second generation SPW-2 and the third generation Wearable 3. Also, the radio is limited to a single standard the BLE. Furthermore, there is an additional accelerometer in the first two generations, which by design they were placed at a distance of 30 mm. They were used to simulate gyroscope functionality by calculating the difference between the two accelerometer values at a particular sample by accounting to the distance between them. The sampling frequency of the first two generations was limited 400 Hz, and the supported measurement ranges were $\pm 2g, \pm 4g, \pm 8g$.

Initially the device was powered by non-rechargeable batteries with the accompanying power regulation. Then for better maintainability and uptime a switch was made to wirelessly charged Lithium-Polymer (LiPo) batteries together with better energy efficiency power management circuitry. A noticeable increase in the efficiency at sleep state was obtained when the battery regulation was switched from LTC3388 to TPS62746. Supplementary to the high efficiency regulator a linear regulator was placed to power the accelerometers which had very good noise performance. The low noise regulator allowed for lower mean root square (rms) noise in accelerometer sampled data.

There were a few design elements that were successful has been migrated over to the current generation. The linear regulator TPS78318 delivering low noise was used both in the SPW-2 and the Wearable 3. The CC260 SoC from SPW-2 was migrated into the new design. This Soc provides more energy efficient wireless connectivity by supporting off-the-shelf radio that both BLE and IEEE 802.15.4 and link layer of 6LoWPAN, ZigBee and Thread.The MX25R6435F flash memory was also migrated. A notable feature is it's ability to consumes very low current of 200 nA in shutdown mode.

3.2 The Third Wearable: Wearable 3

The Wearable 3 features one MC3635 accelerometer. The SPW-1 demonstrated the practical improvements in energy consumption of using a DCDC converter, instead of a linear voltage regulator. However, the output voltage of the switching regulator has a 50 mV periodic fluctuation that introduces noise in the measurements of the MC3635 accelerometers. The Wearable 3 mitigates this issue by incorporating two voltage regulators. The combination of the low-noise linear voltage regulator (TPS78318) and high-efficiency DCDC converter (TPS62746) improves the noise levels of the experiments at the cost of only a minor increase of the power consumption of the accelerometers. The Wearable 3 also uses 3.7V Li-Po Batteries designed to fit a 100 mAh with BQ51013B Qi-compliant [1] wireless power receiver and battery charger. Compared to SPW-2 a change was made in the power management subsystem was the switch from a single wireless power and charging IC in SPW-2 to two separate IC in the Wearable 3. This further decreased leakages of current. A 7.5 μH low-profile (19 mm round up to 0.8 mm) Qi-compliant wireless power receiver coil (WE-WPCC) is chosen for LiPo batteries because of user-friendliness in reloading and low-cost waterproof inclusions of the wearable sensor. The Wearable 3 also includes a gyroscope (ICM-20948) that powered from a GPIO as it requires more power than the accelerometer. The Wearable 3 has 8 MB peripheral flash memory (MX25R6435F) with only 200 nA in shutdown mode. Like SPW-1 and SPW-2, the Wearable 3 employs one button (but unlike in previous devices, the button is capacitive) and one general purpose LED. In the Wearable 3, as in the SPW-2, 5 exposed GPIOs can be connected external sensors to support digital inputs; 3 of them are shared with the SPI bus but also support analogue input. A meandered inverted-F antenna (maximum directivity of 5.3 dBi) that is printed on the FR4 substrate of the Wearable 3 is matched to the differential RF output of the CC2650. The nRF51822 used by SPW-1 allows a transmission power of+4 dBm, whereas CC2650 allows a higher transmission power of +5 dBm. Fig. 2 shows the internal hardware sub-systems diagram of the Wearable 3. Table 1 compares the Wearable 3 with the SPW-1 and SPW-2, summarizing their features.

The Wearable 3 is designed with smaller dimension (i.e., external dimension of 38.5x38.5x12.5 mm and smaller battery size 23.5x17.5x3) compared to the SPW-2 for comfort. The new wearable incorporates 3D compass, which gives better motion capture. A new sensor is also included in the Wearable 3 to measure heart rate. The new Wearable 3 also supports easy comm USB interface. The Wearable 3 has also interface of vibration for tactile haptic feedback, touch button for user interaction, screen for visual information and capable to connect with other interactive platforms. Fig. 3 shows the external diagram of the Wearable 3 interface with USB connector.

Figure 4 shows the wearable device and its minimal implementation components for data collection.

4 Performance Evaluation

BLE radio has 4 times higher symbol rate than the IEEE 802.15.4: 1 Mbps versus 250 Kbps. However, BLE has a 3 dB lower sensitivity on the receiver. From measurements presented below assuming that the BLE requires 3 dB higher power to transmit at the maximum power level of +5 dBm compared to +2 dBm the radio consumes 730 μA or 7.5 % more for the duration of the transmission. The measurements were derived using variable transmit power for a fixed maximum size of BLE advertisements. The duration of the transmission has an inherent offset due to radio setup. By varying

Table 1. Summary of Features of SPW-1, SPW-2 and SPW3

Features	SPW-1	SPW-2	Wearable 3
SoC	nRF51822	CC2650	
BLE	Yes		
IEEE 802.15.4	No	Yes	
Processor	Cortex M0	Cortex M3	
RAM	32KB	30KB	
Internal Flash	256KB	128KB	
Coin Cell Support	Yes		
Li-Po Support	Yes		
Battery Voltage	2.7 – 6 V	2.15 – 5.5 V	
Battery Charger	Yes		
Wireless Power (Qi)	No	Yes	
Energy Awareness	Yes		
Charging Awareness	No	Yes	
Accelerometer	2		1
Gyroscope	No	Yes	
External Flash	No	8MB	
PCB Antenna	Yes		
Max. Directivity	7 dBi	5.3dBi	
Max. Tx Power	+4 dBm	+ 5 dB	
External Antenna	Yes	No	
LED	2	1	
Button	1		
GPIOs	7	5 (SPI)	
Analogue GPIOs	2	3 (SPI)	
Screen	No		Yes

the packet length and looking into the time that the radio is active the start-up time and the time per byte can be derived. Using a linear regression model using variable length packets the radio start-up time is 547.2 μs and 5.38 μs per byte of data.

$$\begin{aligned} t_{tx} &= t_{setup} + t_{rampup} + t_{perbyte} \times bytes + t_{rampdown} \\ &= (239 + 141 + 8 \times bytes + 78)10^{-6}(s) \end{aligned} \quad (1)$$

Measurements shown in Fig. 5 were taken using +5 dBm transmit power. The changes in transmit power affects only the transmission part. For reception and radio setup, ramp up and ramp down the energy expenditure remains the same.

Having two radios transmitting 37 bytes of information. The choice of number is based on the maximum packet size allowed for BLE advertisements. Radio A and B transmitting using BLE and 802.15.4 respectively. B will require 80 % more time to transmit the packet. This equates to 80 % more power at the same power level. If we operate at the limit of the link budget where A has to transmit with 3 dB higher power than B. Then B consumes 67.5 % more power per byte. Fig. 6 shows the BLE energy consumption with variable length. At the same level, 802.15.4 will require 4 time higher power on transmitting the data which leads to the 80 % higher energy at 37 bytes of transmission.

Apart from transmissions reception power must be considered. During reception the micro controller consumes a constant amount of power. Thus the only variable affecting the power consumption is the time radio spends active to receive the information. Using the BLE active scanning mode we can deduce a metric for the receive power mode to assess the reception energy.

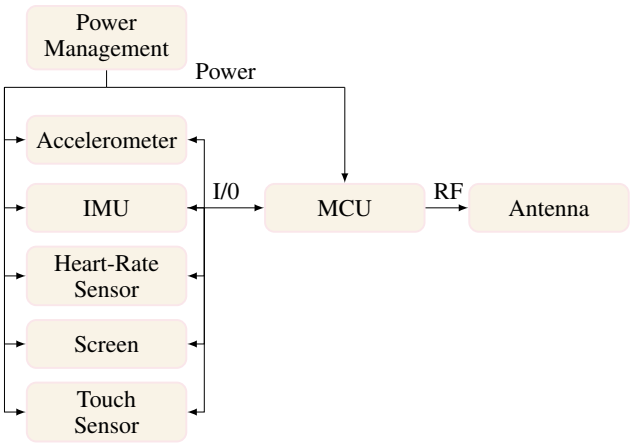

Figure 2. Internal hardware sub-systems of the Wearable 3.

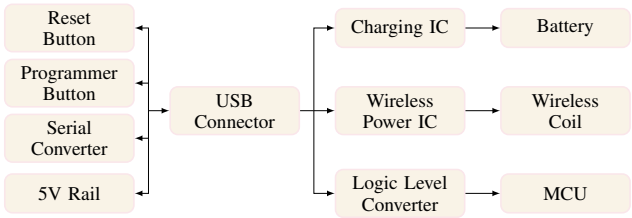

Figure 3. External interfaces of the Wearable 3.

$$\begin{aligned} t_{rx} &= t_{setup} + 3 \times t_{rampup} \\ &\quad + t_{perbyte} \times (bytes_{adv} + bytes_{req} + bytes_{resp}) \\ &\quad + 3 \times t_{rampdown} \end{aligned} \quad (2)$$

$$\begin{aligned} e_{rx} &= e_{setup} + 3 \times e_{rampup} \\ &\quad + p_{tx} \times t_{perbyte} \times (bytes_{adv} + bytes_{req} + bytes_{resp}) \\ &\quad + 3 \times e_{rampdown} \end{aligned} \quad (3)$$

Notice that the time for which the radio is active the MCU is idling. Thus this time can be used for data processing. This time can be quite significant i.e. 1.3 ms while receiving as show in Fig. 7. In this time features can be extracted from the data collection stream. Based on results for SPW-2 from [6] which uses the same MCU spectral processing for up to 15 samples can be done during a 37byte reception using the scan request response method. Using this approach decision can be done on the device based on the incoming data and the processed features. This decision could include changes in data collection. This could include changes in accelerator sampling frequency and range or activity detection thresholds. Also interactive elements can be used such as presenting messages on user screen, generating vibration notifications.

Fig. 8 shows the sleep current distribution for the Wearable 3 that shows efficiency in new power delivery regula-

Figure 4. Top: device on a charger, middle: device internals, bottom: wireless charging receiver.

tors and the utilization of them in the Wearable 3 (maximum of 600 μA current consumption compared to 2 mA current consumption in SPW-2). Note that the figure shows very low quiescent current during idle time (i.e., the value is around 400 nA and with all peripherals in shutdown mode only 200 nA of excess power as found from the datasheets). This is due to the space restrictions when it come to PCB traces clearances with the power planes. The data was collected using a Rocketlogger device. The dual ADC input for current measurements uses a shunt resistor and a switchable transimpedance amplifier. During transients to high currents above a threshold i.e. 4 mA the transimpedance amplifier layout is bypassed using a MOSFET. The low current ADC is used to examine sleep current and the high range ADC input to assess power consumption while the MCU is active. During the switching points noise and false readings are introduced. These are accounted for by statistically detecting outliers and specifying confidence levels using statistics. To

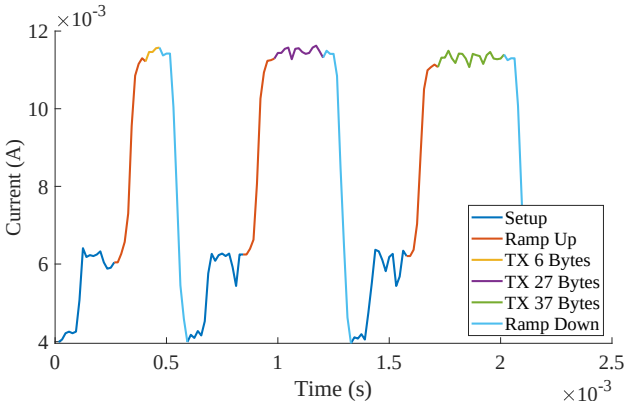

Figure 5. Transmission current consumption at different states.

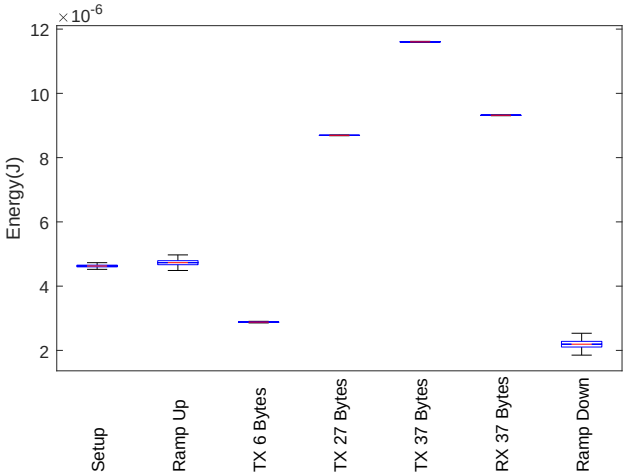

Figure 6. Comparison between energy spend per state.

have better representation of power consumption data and the generation of confidence intervals the data had to be fitted to distributions. The statistical approximation for most of the measurements was the normal or Gaussian distribution as hypothesized by the Central Limit Theorem. To achieve this, a large number of samples were collected. Due to the discrete nature of the data samples, Epanechnikov kernel was used to approximate the cumulative distribution function (CDF) of the data points. From the kernel derived CDF approximation the mean and standard deviation values where derived by converging the inverse CDF at different probabilities. The mean can be found at half way of the values. The standard deviation is the difference of the inverse CDF between two values at each side of the Probability Density function (PDF) with probability difference between them of 0.68.

$$\mu = F^{-1}(0.5) \tag{4}$$

$$\sigma = F^{-1}(.6707) - F^{-1}(.3293) \tag{5}$$

The choice of normal distributions is to allow combinations, additions and subtractions of different power consumption states. The combination of those could provide a figure of the expected battery life with the corresponding confidence intervals. Millions of samples of the sleep current for different

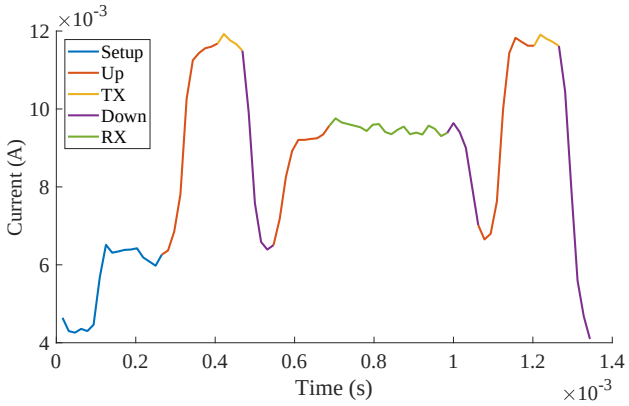

Figure 7. Comparison between energy spend per state during reception.

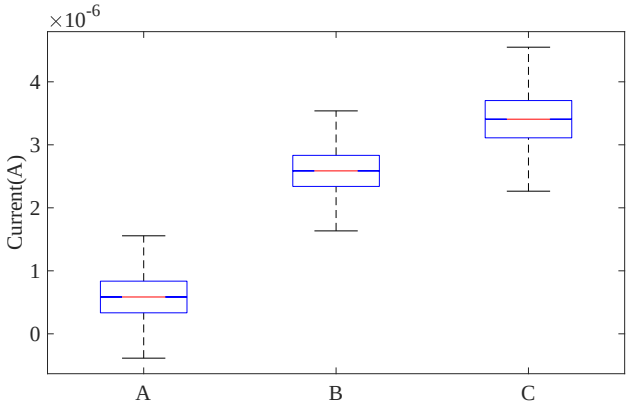

Figure 8. Power consumption differences in idle. State A: device sleeping, State B: accelerometer enabled, State C: accelerometer and touch button enabled.

states were collected to generate confidence intervals. The sleep current was measured while having occasional wake up calls. To account for current transients and isolate the regions of interest the data was represented using normal distributions. The lowest power state is where the MCU input outputs are set to the lowest leakage setting. The MCU can only wake up from timers set prior to sleeping. This represents state A on Fig. 8. The next state is when the accelerometer is on and sampling data at 28 Hz. The last state is when both the accelerometer and the touch sensor IC are both on. Notice that the variance of the state C is larger than A and B due to the fact that the touch sensor its an independent current sink. Thus, the outcome is the sum of two normally distributed random variables. Also this indicates that the low noise circuity implemented for the accelerometer does not have any current noise thus no voltage noise. Another important information that can be derived from Fig. 8 is the cost of adding user interaction on the device. An accelerometer and the touch button can provide interrupts to the MCU. Using these interrupts, the MCU is able to wake up and present screen messages to the user. The capacitive button allows to wake up the screen and to navigate across menus, while the accelerometer can provide gesture detection. This dual interaction potential can be enabled with current consumption as low as 3.4 μA (Fig. 8).

5 Conclusion and Future Work

This paper presents the Wearable 3, a new wrist-worn sensor node for residential monitoring, and evaluates its performance. We show that by using two way communication with bidirectional RSSI information exchange for accessing network utilization, the Wearable 3 can potentially reduce the number of BLE channels used for advertisement messages from 3 to 1, i.e., 66 % energy savings in transmission compared with the previous version. The paper also presents various energy measurements, including the minimum energy required for receiving data using BLE *scan request / scan response* approach. In addition, this paper identifies a region where data processing can be done: i.e., while waiting for the RF queues to be emptied. In the future, additional sensor functionality can be incorporated in the design by utilizing the flex connector on-board. A mixed signal interface with flexible PCBs or board-to-board connections allows the device to connect with ECG, pulse oximetry, and other sensors.

6 Acknowledgments

This work was performed under the SPHERE Next Steps Project funded by the UK Engineering and Physical Sciences Research Council (EPSRC), Grant EP/R005273/1. It was also supported by the ERDF Activity 1.1.1.2 “Post-doctoral Research Aid” (No. 1.1.1.2/VIAA/2/18/282).

7 References

[1] bq51013B Highly Integrated Wireless Receiver Qi (WPC v1.2) Compliant Power Supply. http://www.ti.com/lit/ds/symlink/bq51013b.pdf.

[2] S. Adibi. Link technologies and blackberry mobile health (mhealth) solutions: A review. *Information Technology in Biomedicine, IEEE Transactions*, 16(4):586–597, 2012.

[3] I. Biswas and B. Walker. Psychofizz – real-time monitoring of physiological traits over wireless networks. *Int’l J. of Communications, Network and System Sciences (IJCNS)*, 1(2), 2 2011.

[4] J. Cheng, X. Chen, and M. Shen. A framework for daily activity monitoring and fall detection based on surface electromyography and accelerometer signals. *IEEE J. Biomed. Health Inf.*, 17(1):38–45, 2013.

[5] A. Elsts, X. Fafoutis, G. Oikonomou, R. Piechocki, and I. Craddock. TSCH Networks for Health IoT: Design, Evaluation and Trials in the Wild. *ACM Transactions on Internet of Things*.

[6] A. Elsts, R. McConville, et al. On-board feature extraction from acceleration data for activity recognition. In *EWSN*, pages 163–168, 2018.

[7] X. Fafoutis, B. Janko, et al. SPW-1: A Low-Maintenance Wearable Activity Tracker for Residential Monitoring and Healthcare Applications. In *HealthWear*, 2016.

[8] X. Fafoutis, A. Vafeas, et al. Designing wearable sensing platforms for healthcare in a residential environment. *EAI Endorsed Transactions on Pervasive Health and Technology*, 17(12), 9 2017.

[9] P. Gupta and T. Dallas. Feature selection and activity recognition system using a single triaxial accelerometer. *IEEE Trans. Biomed. Eng*, 61(6):1780–1786, 2014.

[10] D. A. James and N. Petrone. *Sensors and Wearable Technologies in Sport*. SpringerBriefs in Applied Sciences and Technology. Springer Singapore, 2016.

[11] H. Qiu, X. Wang, and F. Xie. A survey on smart wearables in the application of fitness. In *DASC/PiCom/DataCom/CyberSciTech*, pages 303–307, Nov 2017.

[12] L. Sigrist, A. Gomez, R. Lim, S. Lippuner, M. Leubin, and L. Thiele. Rocketlogger: Mobile power logger for prototyping iot devices: Demo abstract. In *ACM SenSys*, pages 288–289. ACM, 2016.

[13] J. Winkley, P. Jiang, and W. Jiang. Verity: an ambient assisted living platform. *IEEE Transactions on Consumer Electronics*, 58(2):364–373, 2012.